Delft University of Technology
Department of Aerospace Engineering

Report LR-414

A CURVED TEST SECTION FOR RESEARCH ON TRANSONIC SHOCK WAVE-BOUNDARY LAYER INTERACTION

C. Nebbeling
W.J. Bannink

Delft - The Netherlands

January 1984

Delft University of Technology
Department of Aerospace Engineering

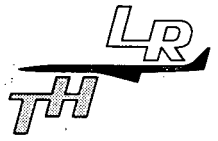

Report LR-414

A CURVED TEST SECTION FOR RESEARCH ON TRANSONIC SHOCK WAVE-BOUNDARY LAYER INTERACTION

C. Nebbeling
W.J. Bannink

Delft - The Netherlands

January 1984

ACKNOWLEDGEMENT

The authors are particular grateful to mr. E.W. de Keizer and ir. M. van Lent for the development of the automatic choke control.

SUMMARY

This report describes the design of a nozzle with a curved test section for a blow-down wind tunnel. The purpose of such a nozzle is the generation of a transonic flow to investigate shock wave-boundary layer interaction on a convex curved wall at the lower side of the test section. The ratio of the thickness of the oncoming boundary layer and the radius of curvature of the convex wall corresponds to free flight conditions of transonic civil aircraft. For this ratio a value of 80 has been taken in the present design, which leads, with an estimated boundary layer thickness of 5-6 mm, to a radius of curvature of 450 mm. The supersonic pocket occurring on the convex wall which does not extend to the upper wall of the nozzle is terminated by a shock wave. The Mach number at the lower wall just in front of the shock wave may be varied between $M = 1.2$ and $M = 1.45$. The Mach number at the concave upper wall does not exceed $M = .85$. The flow through the test section is regulated by an automatic, computer controlled choke mechanism, the input being the pressure difference across the shock wave.
Preliminary measurements using the present design show the usefulness of the application of a simple one-dimensional analysis to determine the cross-sectional area distribution of the nozzle, the Mach number and pressure distribution in front of the shock wave and the dimensions of the downstream choke area.
The measurements confirm that the ultimate design meets the requirements.

CONTENTS

LIST OF SYMBOLS

a^* critical speed of sound

h distance normal to the lower wall at the position of the shock wave-boundary layer interaction

h_c^* height of the downstream choke section

h_m heigth of the test section at the position of the shock wave-boundary layer interaction

h^* height of the upstream critical cross-sectional area

M local Mach number

p pressure

p_t total pressure

$\bar{p}$ non-dimensional pressure, $\frac{p}{p_t}$

r local radius of curvature of a streamline

R radius of curvature of the wall

u local flow velocity

δ_o boundary layer thickness at the convex wall, just ahead of the interaction region

γ ratio of specific heats

ρ density

ρ^* critical density

Subscripts:

1 upstream of shock wave

2 downstream of shock wave

ℓ lower convex wall

u upper concave wall

w at the lower wall just ahead of the shock wave

1. INTRODUCTION

The interaction of a shock wave and a turbulent boundary layer at the upper side of an aerofoil occurs in general at a curved surface. In 1973 Bradshaw (Ref. 1) argued that wall curvature is an essential parameter for a turbulent boundary layer, since it may influence the eddy visocity significantly and therefore play an important role in the interaction process.

In the literature on the subject one finds that a majority of experimental investigations has been devoted to the interaction on a plane surface (Refs 2-8). The first detailed and concise study is dated as far back as 1946, when Ackeret, Feldmann and Rott (Ref. 9) made their famous experiments on shock wave-boundary layer interaction on a curved surface. The emphasis of Ref. 9 was laid on the influence of the Reynolds number on the interaction process. It was observed that in the case of a laminar boundary layer a λ-type shock wave existed at fairly low Mach numbers ($\approx$1.11). The corresponding pressure distribution along the wall showed a smooth and gradual behaviour. At similar Mach numbers and a turbulent boundary layer no such λ-type shock was found and the pressure distribution along the wall in the interaction region appeared to be much steeper than in the laminar case. Ackeret et al. did not investigate the influence of wall curvature on the interaction process.

Another well known experiment on shock wave-turbulent boundary layer interaction, however on a plane wall and at the rather high Mach number of 1.47 at the foot of the shock wave, was made by Seddon (Ref. 2). In his case a λ-type shock wave was observed with a small downstream region of supersonic flow (supersonic tongue) accompanied by a separated turbulent boundary layer downstream of the shock. Although the occurrence of a λ-shock was confirmed by Vidal (Ref. 3), East (Ref. 4) and Kooi (Ref. 5) there was a significant difference: the supersonic tongue did not appear at a Mach number of 1.40 and the separation bubble was hardly present; also the shape of the supersonic tongue differed considerably from the one given by Seddon.

All these phenomena have been observed at plane surfaces but it is worthwhile to incorporate also the influence of wall curvature, since, form the point of view of the shape of aerofoils, such a surface appears to be somewhat more realistic. In order to meet the requirements of wall curvature in the laboratory a special design has been developed described in the present report. The design consists of a curved transonic test section in which on the lower convex tunnel wall a local supersonic region may be generated, terminated by a shock wave, see Fig. 1. The Mach number at the wall just ahead of this shock wave may be varied between 1.2 and 1.45 by changing the extent of the supersonic region, which is

achieved by varying the cross-sectional area of a downstream choke.

For a fixed wall curvature the ratio of the radius of curvature R and the boundary layer thickness δ_o in front of the shock wave may be varied by influencing δ_o. The latter could be achieved by variation of the tunnel stagnation pressure, by application of surface roughness or by air injection.

The present report contains criteria and calculations for the actual design of the curved channel.

2. DESIGN OF THE CURVED CHANNEL

2.1. Modification of an existing blow-down wind tunnel

As a basis for the design the supersonic blow-down wind tunnel, ST15, of the Laboratory for High Speed Aerodynamics, Department of Aerospace Engineering of the Delft University of Technology , has been selected (Fig. 2). This tunnel is equipped with nozzle blocks which can easily be interchanged. The width of the channel is 15 cm and the height between upper and lower girder is 40 cm. Since the side walls can completely be removed, the accessability of the tunnel is such that any desired nozzle block may be installed without difficulty.
Flow visualization is possible through the large windows (dia. 25 cm) in the side walls. Downstream of the test section there is an adjustable probe support mechanism, driven by electric stepping motors, which allows the possibility to explore the flow field by means of fine measuring probes (Fig. 3). Also the boundary layer at the tunnel walls may be influenced artificially without severe restrictions of the tunnel construction.
The maximum allowable pressure in the test section is 2.5 bar, imposing an upper limit to the Reynolds number of 7.10^5 per cm, by variation of the tunnel stagnation pressure.

2.2. Design considerations

In order to simulate in the laboratory the transonic shock wave-boundary layer interaction process as it occurs in real flight conditions of modern transonic aircraft, the Reynolds number based on the boundary layer thickness, the boundaries of the flow field and the pressure distribution upstream and downstream of the interaction region are parameters of major importance that should be simulated as good as possible.
For this reason in the planned investigation the ratio of the boundary layer thickness just ahead of the shock wave and the radius of curvature of the wall at that position was taken such that it corresponds to free flight conditions; according to Ref. 10 a value of R/δ_o between 50 and 100 might fulfil this requirement. In the present design $R/\delta_o = 80$ has been chosen.
Then, the boundary layer thickness at the convex (lower) wall of the tunnel channel becomes a determining factor for the radius of curvature to be selected. Preliminary measurements (Ref. 11) have shown that the boundary layer thickness

at a position where the interaction is due to occur might be 5-6 mm. The contour in the present design will not be the same as that of Ref. 11. However, it is expected that a different contour will not affect the boundary layer thickness significantly. Therefore the boundary layer thickness δ_o is taken as 5.5 mm, resulting in a radius of curvature of the lower wall of R = 450 mm.

2.3. Estimate of the normal pressure distribution in the test section in relation to wall curvature

The dimensions of the test section will be determined in terms of a maximum Mach number of 1.45 at the lower wall just upstream of the shock wave. This value has been chosen since it represents about the highest Mach number that occurs at the foot of the shock wave terminating the supersonic region on transonic aerofoils of modern civil aircraft.

The Mach number at the (concave) upper wall is taken to be 0.85. The criterium underlying this value is found in a save margin of subsonic flow along the upper wall in order to circumvent the possibility of centred supersonic disturbances from the concave upper wall which run into the shock wave. Such a flow phenomenon might distort the concept of an isolated supersonic pocket on the lower wall.

At the position where the interaction is due to occur the velocity distribution normal to the convex wall and the height h_m of the test section at that position is determined from the normal pressure gradient

$$\frac{dp}{dr} = \frac{\rho u^2}{r} = \frac{\gamma M^2 p}{r} \qquad (1)$$

where p is the pressure, ρ the density, u the local velocity along a streamline, M the Mach number and r the local radius of curvature of a streamline.

Introducing the non-dimensional pressure $\bar{p} = \frac{p}{p_t}$, where p_t is the total pressure, we obtain with $\bar{p} = \left(1 + \frac{M^2}{5}\right)^{-7/2}$ $(\gamma = 1.4)$

$$\frac{d\bar{p}}{\bar{p}} = 7\,\frac{1-\bar{p}^{2/7}}{\bar{p}^{2/7}}\,\frac{dr}{r} \qquad (2)$$

Eq. (2) may easily be integrated yielding

$$\bar{p} = [1 - (\frac{A}{r}\frac{r_{ref}}{})^2]^{2/7} \tag{3}$$

where A and r_{ref} are integration constants. If for r_{ref} is taken the radius of curvature, R_ℓ, of the lower (convex) wall we then have at the wall

$$\bar{p}_w = (1 - A^2)^{7/2} = (1 - \frac{M_w^2}{5})^{-7/2} \tag{4}$$

where M_w is the Mach number at the lower wall at the streamwise position where the normal pressure distribution is considered, that is: just in front of the shock wave-boundary layer interaction.
From Eq. (4) the constant A is found to be

$$A = (\frac{M_w^2}{M_w^2 + 5})^{1/2} \tag{5}$$

Then the normal pressure distribution becomes

$$\bar{p} = [1 - \frac{M_w^2}{M_w^2 + 5} (\frac{R_\ell}{r})^2]^{7/2} \tag{6}$$

For a given radius of curvature, R_ℓ, of the lower wall and a desired Mach number M_w, the pressure distribution may now be calculated as a function of the distance h normal to the wall, assuming that the local radius of curvature r varies linearly with h as

$$r = R_\ell + \frac{h}{h_m} (R_u - R_\ell) \tag{7}$$

In Eq. (7) h_m is the height of the test section (the distance between upper and lower wall) at the shock wave position, $0 \leq h \leq h_m$; R_u is the radius of curvature of the upper wall.

Eq. (6) then reduces to

$$\bar{p} = \left[1 - \frac{M_w^2}{M_w^2 + 5}\left\{1 + \frac{h}{h_m}\left(\frac{R}{R_\ell} - 1\right)\right\}^{-2}\right]^{7/2} \qquad (8)$$

In the cross-sectional plane where the interaction is due to occur we have at the upper wall at $M = 0.85$, $\bar{p} = 0.6235$ and at the lower wall $R_\ell = 450$ mm, $M_w = 1.45$. Then, for the radius of curvature of the upper wall we find $R_u = 690$ mm (in the actual design $R_u = 700$ mm has been taken, resulting in a Mach number at the upper wall of 0.84).

The only unknown quantity in Eq. (8) is the height h_m of the test section. h_m will be determined in the following paragraph.

2.4. Height of the test section

The heigth of the test section has to be determined within constraints of the tunnel construction.

The first constraint is the mass flow through the regulation valve of the tunnel; the maximum effective cross-sectional area of this valve is 35 cm^2. The minimum pressure in the air supply system of the laboratory is 10 bar, this requirement is put by auxillary apparatus. Preliminary channel designs (Ref. 11) showed that an average value of the static pressure in the test section of 1 bar was necessary to sustain a transonic flow. This means that the maximum cross-sectional area of the test section could be 350 cm^2; thus for a width of the tunnel channel of 15 cm the height of the test section should not exceed 23 cm.

A second constraint for h_m is set by the dimensions of the diffusor downstream of the free jet chamber of the tunnel. Fig. 3 shows the construction of the diffusor and the support for the probe traversing mechanism; the length of the free jet chamber is 300 mm. In order to determine h_m, the losses in total pressure in the flow between the test section and the diffusor should be known. The flow process proceeds as follows: from the settling chamber the flow accelerates up to the normal shock wave in the test section. Downstream of the shock wave the subsonic flow accelerates to sonic conditions in the choke section at the end of the tunnel channel (Fig. 4). After the choke the flow

immediately enters into the free jet chamber, where it is accelerated to supersonic speeds until a normal shock wave is formed in the diffusor entrance. In the diffusor throat again sonic conditions are reached. The flow enters the free jet chamber with a divergence angle of 7° (Ref. 12). The diffusor entrance is constructed as a bell mouth, conform Ref. 12, in order to achieve an effective capturing of the free jet. The diffusor has a constant width of 150 mm and the height of its throat is 180 mm.

Since the sonic choke exit acts as a first throat of the flow, its cross-sectional area is certainly less then that of the diffusor throat. In the starting process of the windtunnel flow, a shock wave might to be swallowed by the diffusor. Therefore for fixed dimensions of the diffusor the height of the sonic choke exit has to be determined such that swallowing is possible. The calculation of this height has been done in an iterative way, as a result a height of 165 mm has been obtained. During the starting process, the free jet expands with the above mentioned divergence of 7° and enters the diffusor where the shock wave to be swallowed is formed at a streamwise position where the boundaries of the jet meet the diffusor wall (similar to Ref. 12 a one-dimensional analysis is considered). From the dimensions and geometry of the free jet chamber and the diffusor, shown in Fig. 4, it follows that the initial shock position in the converging part of the diffusor will be at 286 mm downstream of the choke exit at a Mach number of 1.54.

At this Mach number the ratio of total pressures across the shock wave is 0.9166 which brings the height of the choke at .9166 * 180 = 165 mm, as mentioned above. This height of the choke exit is taken as a basis for the determination of the heigth h_m of the tunnel test section at the position of the shock wave-boundary layer interaction.

The Mach number distribution across the test section in vertical direction is obtained from Eq. (8), for $M_w = 1.45$, $R_\ell = 450$ mm, $R_u = 700$ mm we obtained

$$M = [5(\bar{p}^{-2/7} - 1)]^{1/2} \tag{9}$$

The local losses in total pressure across the shock wave are determined by

$$\frac{p_{t_2}}{p_{t_1}} = \left(\frac{6M^2}{M^2+5}\right)^{7/2} \left(\frac{6}{7M^2-1}\right)^{5/2} \tag{10}$$

We may now form the continuity of mass between the test section and the downstream sonic choke section, namely

$$\int_0^{h_m} \rho u \, dh = \int_0^{h^*_c} \rho^*_c \, a^* \, dh_c \tag{11}$$

where h^*_c is the total height of the sonic choke cross-sectional area and ρ^*_c and a^* are the critical density and speed of sound, respectively, in this section.

As may be computed from Eqs (8) and (9) the shock wave in the test section extends to a height of $0.6\ h_m$, the rest of the cross-section being subsonic.

Now the mass flow given by Eq. (11) is divided into two parts: one part flowing through the shock wave is subjected to losses in the total pressure, the other part remains entirely subsonic and reaches the sonic speed in the choke cross-section.

For the mass flow through the shock wave we may write

$$\int_0^{h^*_{c_\ell}} \rho^*_{c_\ell} \, a^* \, dh_c = h_m \int_0^{0.6} \rho_2 \, M_2 \, a_2 \, d\left(\frac{h}{h_m}\right) \tag{12}$$

where $h^*_{c_\ell}$ is the part of the sonic choke cross-section covered by the mass flow through the shock wave and $\rho^*_{c_\ell}$ is the critical density in this part; the subscript 2 in the right hand side of the equation denotes the condition just behind the shock wave in the test section. Eq. (12) may be reduced to

$$h^*_{c_\ell} = \frac{\rho_{t_2}}{\rho^*_{c_\ell}} \sqrt{\frac{T_t}{T^*_{c_\ell}}} \, h_m \int_0^{0.6} \frac{\rho_2}{\rho_{t_2}} \, M_2 \sqrt{\frac{T_2}{T_t}} \, d\left(\frac{h}{h_m}\right)$$

The integrand is a function of the Mach number just ahead of the shock wave. Numerical integration yields

$$h^*_{c_\ell} = 0.585 \, h_m \tag{13}$$

In the second, complete subsonic, part of the mass flow we have

$$\rho^*_{c_u} \; a^* \; h^*_{c_u} = h_m \int_{0.6}^{1} \rho \; M \; a \; d\left(\frac{h}{h_m}\right) \qquad (14)$$

where $h^*_{c_u} = h^*_c - h^*_{c_\ell}$, $\rho^*_{c_u}$ is the critical density and the integrand is taken in the upper part of the test section.

Reduction of Eq. (14) leads to

$$h^*_{c_u} = \frac{\rho_t}{p^*_{x_u}} \sqrt{\frac{T_t}{T^*_{c_w}}} \; h_m \int_{0,6}^{1} \frac{\rho}{\rho_t} \; M \sqrt{\frac{T}{T_t}} \; d\left(\frac{h}{h_m}\right)$$

This integral may be evaluated also, yielding

$$h^*_{c_u} = 0.396 \; h_m \qquad (15)$$

Since $h^*_{c_\ell} + h^*_{c_u} = h^*_c = 165$ mm, there follows that

$$h_m = 168.2 \text{ mm}$$

The distribution of the various flow parameters across the test section just ahead of the shock wave are given in Figs 5, 6 and 7: the pressure in Fig. 5a, the Mach number in Fig. 5b, the losses in the total pressure across the shock wave in Fig. 6 and the specific mass flow in fig. 7.

3. DESIGN OF THE TOTAL NOZZLE

For the experimental investigation of the shock wave-boundary layer interaction it is necessary to visualize the interaction region to an extent as large as possible. Therefore, the design should be such that the major part of the lower (convex) wall is covered by the existing optical system.

The upstream part of the nozzle has to fit to the settling chamber exit with a height of 360 mm.

To determine the static pressure at this cross-section the critical height h* for this flow is required. The value of h* may be determined using the losses in total pressure across the shock wave, the height of the choke and the height of the test section.

Integration of Eq. (10) from zero to $0.6\, h_m$ results in a mean value of $p_{t_2}/p_{t_1} = .9870$.

Since

$$h^*_\ell = .9870\ h^*_{c_\ell} \quad \text{and} \quad h^*_u = h^*_{c_u} = 0.396\ h_m = 66.6 \text{ mm}$$

where the subscripts ℓ and u stand for lower and upper, respectively, or, the parts of the upstream flow passing through the shock wave and passing above the shock wave, h^*_ℓ results from:

$$h^*_\ell = (165 - 0.396\ h_m)\ 0.987 = 97.1 \text{ mm}$$

The total critical height of the subsonic flow in front of the shock wave now becomes:

$$h^* = 163.77 \text{ mm}$$

With this critical height, h*, the pressure p/p_t at the entrance of the nozzle is known.

In order to obtain a gradual development of the boundary layer at the lower wall, its contour is chosen in such a way that it changes only very gradually from the concave curvature near the settling chamber into the convex curvature of the test section.

The development of the boundary layer at the upper wall is considered to be of

less importance, except that the possibility of separation should be avoided. This leads to criteria for the mean streamwise pressure distribution and therefore for the cross-sectional area distribution.

In order to minimize the probability of flow separation the mean pressure gradient is chosen as low as possible, such that a smooth continuous contour could be obtained. The cross-sectional area distribution in the subsonic part of the nozzle was obtained from the relations for compressible flow, giving for each p/p_t value the height in terms of h/h^* at a constant tunnel width.

As soon as partially a supersonic flow occurs the subsonic part and the supersonic part of the flow have to be considered separately to determine the value of the mean pressure belonging to the cross-sectional area. To calculate the streamwise mean pressure distribution the dimensions of the supersonic area have to be known. To acquire reliable information about this point preliminary investigations have been made, which resulted in surface pressure distributions (Fig. 8) and the shape of the embedded supersonic area indicated by disturbances from plastic tape strips at the surface, see the shadow picture of Fig. 9.

Taking into account the above mentioned considerations, the resulting mean pressure distribution and the related cross-sectional area distribution are given in Figs 10 and 11.

Based on the cross-sectional area distribution the contour of the upper wall upstream of the test section is determined, since the contour of the lower wall is already known.

The shaping of the nozzle part downstream of the test section is mainly prescribed by the vertical position of the choke section.

To provide downstream of the shock wave a further compression of the subsonic flow over a certain distance, the height of the nozzle should increase before the acceleration to sonic velocity in the choke starts. The length of the compression zone was chosen about 200 mm to obtain a flow near the interaction comparable to that on an airfoil. The divergency of the nozzle downstream of the shock wave has been deduced from windtunnel surface pressure measurements (Fig. 12) made at a NACA 0012 airfoil at transonic speed in the TST27 windtunnel of the Department of Aerospace Engineering, University of Technology Delft.

The shape of the last part of the nozzle was mainly determined by the constraints of the windtunnel, i.e. the location of the choke. The contour upstream of the choke was made as smooth as possible. Due to the favourable pressure gradient in that part of the nozzle the boundary layer was expected to behave normally. The actual contouring is also based on constructional requirements and is shown in Fig. 13.

The actual choke height can be varied by means of an automatic computer

controlled device which acts on the pressure difference across the shock wave in the test section. Determined by the input of the prescribed pressure difference the strength (position) of the shock wave can be selected at a definite value. Perhaps more important may be the possibility to maintain the shock wave at that well defined position during the traverses of the measuring probe, since its support passes through the choke section, influencing the effective choke area. During the first tests with the designed nozzle the position of the shock wave was maintained within 0.5 mm.

4. RESULTS

Some preliminary tests were performed to check the operation of the facility. In particular the utility of the choke section at the end of the channel as a means to control the Mach number at the foot of the shock wave had to be considered. As the first tests indicated the adjustable choke appeared to be a good device to vary the Mach number in front of the shock wave. The flow was studied using a shadowgraph method with a spark exposure as a light source. On the lower wall in the supersonic region a series of weak disturbances emanates from pressure orifices, as shown in Fig. 14. The Mach number distribution was then determined from these disturbances; this could be done with good accuracy since the quality of the pictures is high. The Mach number distribution across the test section is given in Fig. 15 for the choke adjustment at which the Mach number just in front of the shock wave appears to be 1.52. Since the photograph shown in Fig. 14 was made at an estimated choke setting the design Mach number of 1.45 was not obtained exactly. At the time when this photograph was taken, the automatic control of the shock wave position by means of pressures measured at the lower wall was not yet present. However, the results show a good agreement with the predicted distribution, albeit that they are shifted to a higher Mach number; the actual shock wave position was further downstream than the design position. The nature of the flow appears to be rather insensitive to shock wave position, so that the design Mach number distribution may be obtained within great accuracy. This is the more so because in the case shown in Fig. 14 the supersonic flow is very smooth and free of distinct disturbances.

In conclusion the present simple design provides a suitable adaptation of the nozzle in a blow-down wind tunnel to study locally the important phenomena of transonic shock wave-boundary layer interaction on a curved wall.

5. REFERENCES

1. Bradshaw, P., Effects of Streamline Curvature on Turbulent Flow, AGARDograph 169, August 1973.

2. Seddon, J., The Flow produced by Interaction of a Turbulent Boundary Layer with a Normal Shock Wave of Strength Sufficient to Cause Separation, ARC R&M 3502, 1960.

3. Vidal, R.J., et al., Reynolds Number Effects on the Shock Wave Turbulent Boundary Layer Interaction at Transonic Speeds, AIAA Paper 73-661, 1973.

4. East, L.F., The Application of a Laser Anemometer to the Investigation of Shock Wave Boundary Layer Interaction, AGARD-CP-193, 1976.

5. Kooi, J.W., Experiment on Transonic Shock-Wave Boundary Layer Interaction, AGARD-CP-168, 1975.

6. Gadd, G.E., Interactions Between Normal Shock Waves and Turbulent Boundary Layers, ARC 22, 559-F.M.3051, 1961.

7. Mateer, G.G., et al., A Normal Shock Wave Turbulent Boundary Layer Interaction at Transonic Speeds, AIAA Paper 76-161, 1976.

8. Padova, C., Falk, T.J., Transonic Shock Wave Boundary Layer Interactions, AFOSR-TR-80-0694, 1980.

9. Ackeret, J., Feldmann, F., Rott, N., Untersuchungen an Verdichtungsstössen und Grenzschichten in schnell bewegten Gasen. Bericht Nr. 10 a.d. Inst. f. Aerodynamik ETH, Zürich, 1946.

10. Inger, G.R., Transonic Shock-Turbulent Boundary Layer Interaction and Incipient Separation on Curved Surfaces, AIAA Paper 81-1244, 1981.

11. Sikkes, E.G., De Interactie tussen een Schokgolf en een Turbulente Grenslaag op een Convexe Wand, Afdeling der Luchtvaart- en Ruimtevaarttechniek, Technische Hogeschool Delft, Afstudeerverslag, 1982.

12. Hermann, R., Diffuser Efficiency and Flow Process of Supersonic Wind Tunnels with Free Jet Test Section, AFTR-6334, 1950.

FIGURES

1. Shock wave-boundary layer interaction in a curved test section.
2. Wind tunnel with adapted nozzle contours.
3. Free jet chamber with probe support.
4. Diffusor geometry and shock wave position during starting process of the wind tunnel.
5. Calculated flow parameters across the test section just ahead of the shock wave;
   a. Mach number distribution,
   b. Pressure distribution.
6. Total pressure losses across shock wave in test section.
7. Specific mass flow through the test section.
8. Surface pressure distribution.
9. Schlieren picture of curved transonic flow with shock wave-boundary layer interaction.
10. Mean streamwise pressure distribution in the nozzle at a maximum Mach number of 1.45 m in front of the shock wave.
11. Cross-sectional area distribution of the nozzle.
12. Surface pressure distribution of NACA-0012 profile.
13. Scheme of nozzle showing test section and choke.
14. Transonic shock wave-boundary layer interaction with artificial disturbances.
15. Mach number distribution obtained from the intersections of disturbances of fig. 14.

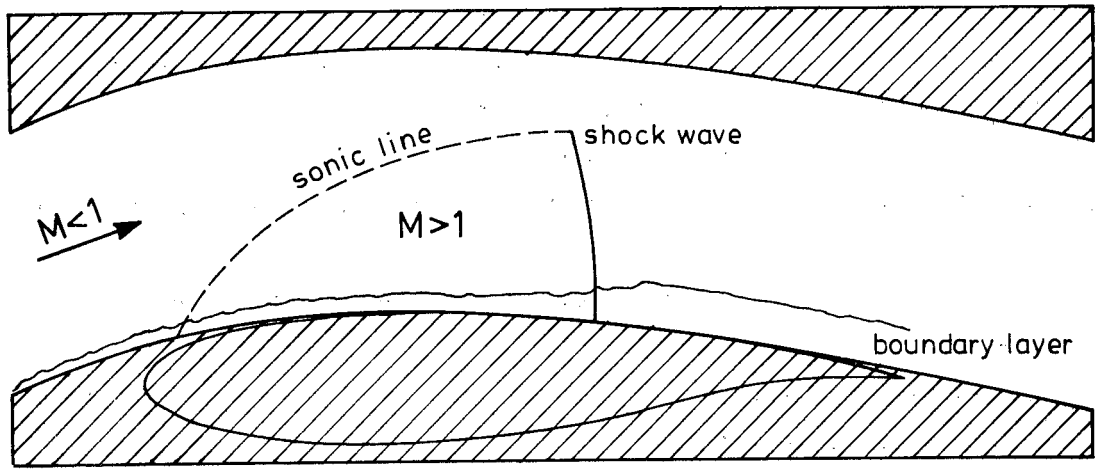

Fig. 1: Shock wave - boundary layer interaction in a curved test section

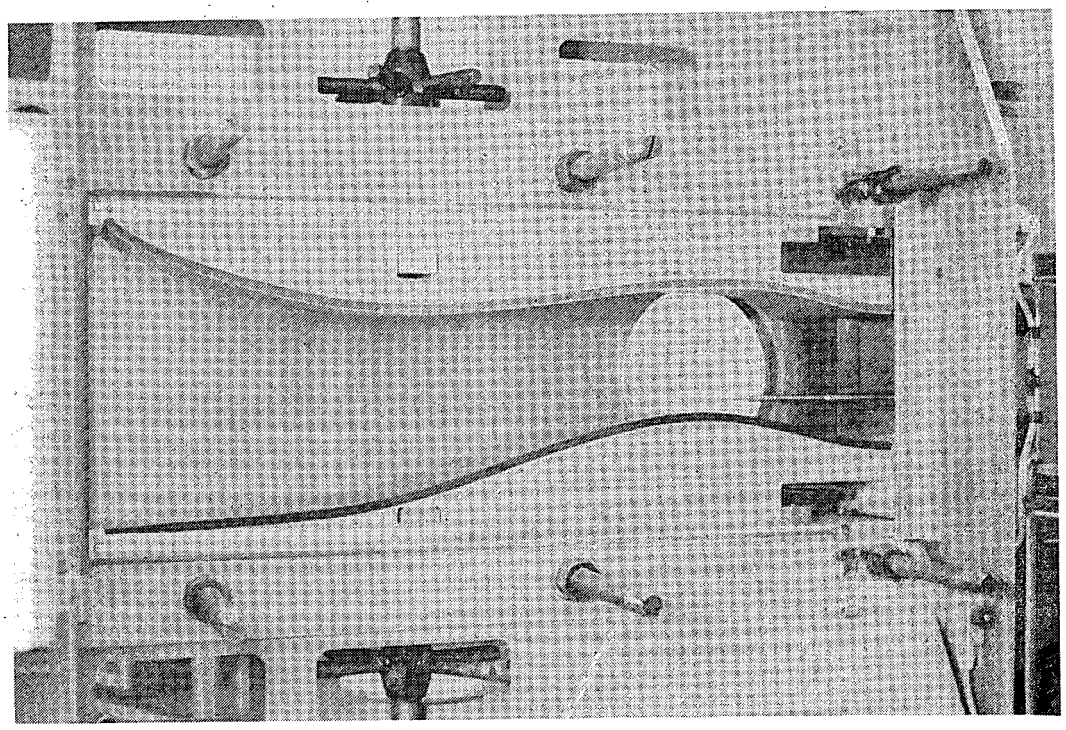

Fig. 2 : Wind tunnel with adapted nozzle contours

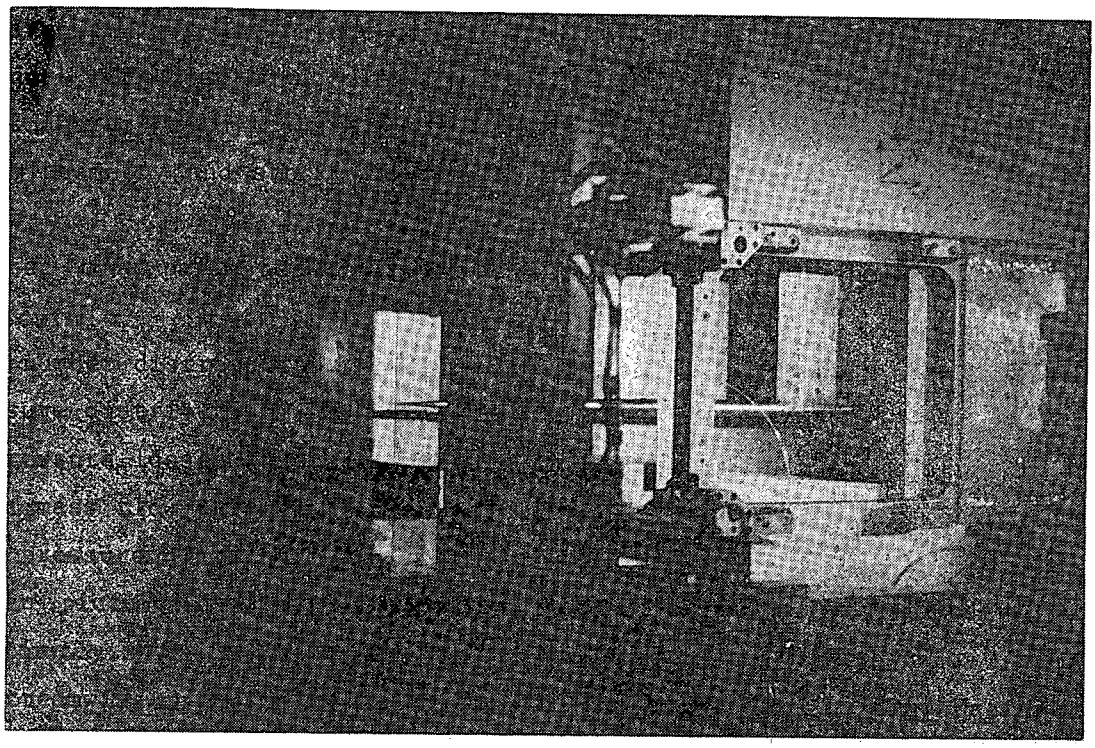

Fig. 3 : Free jet chamber with probe support

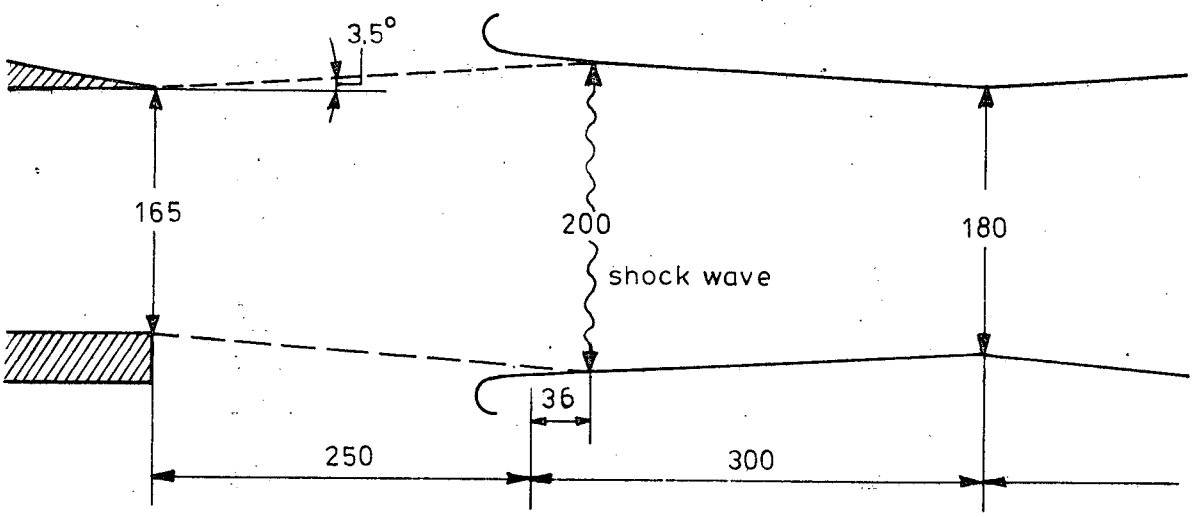

Fig. 4 : Diffusor geometry and shock wave position during starting process of the wind tunnel.

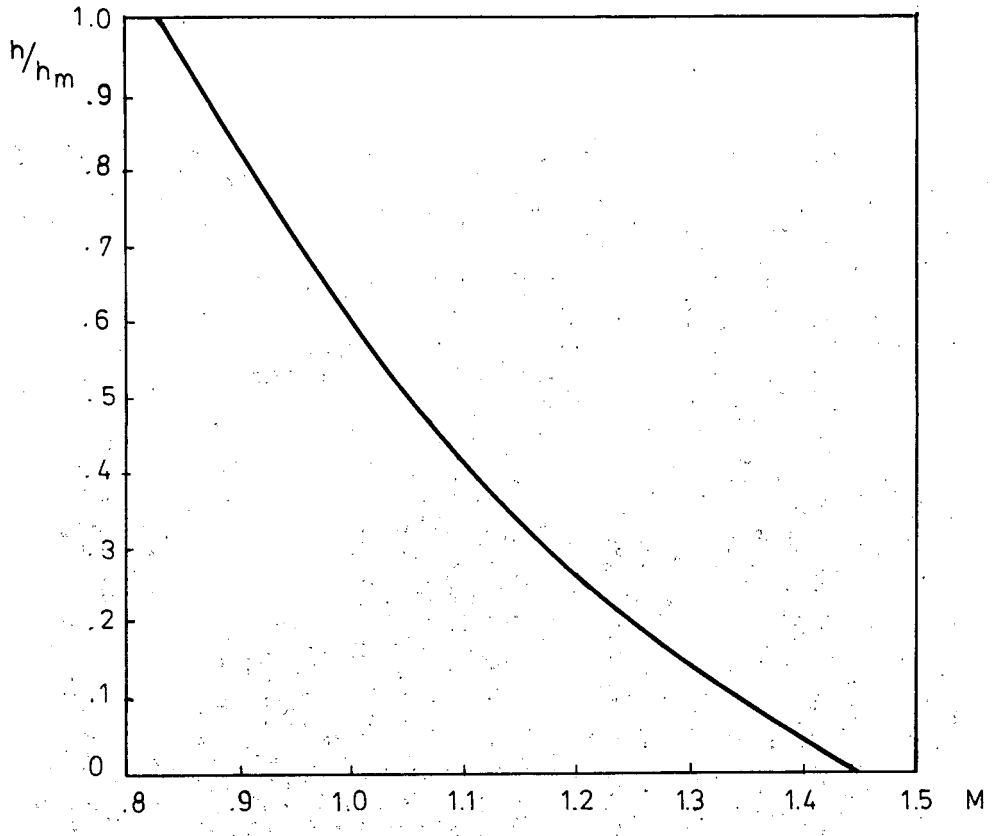

a. Mach number distribution.

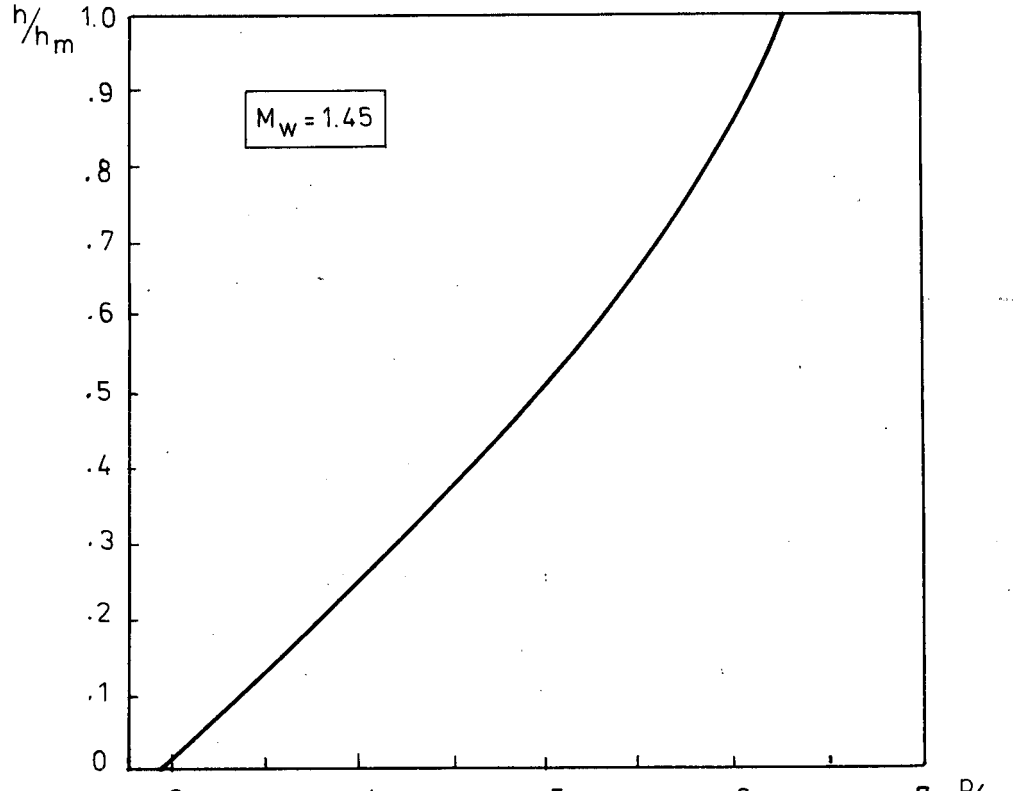

b. Pressure distribution

Fig. 5 : Calculated flow parameters across the test section just ahead of shock wave.

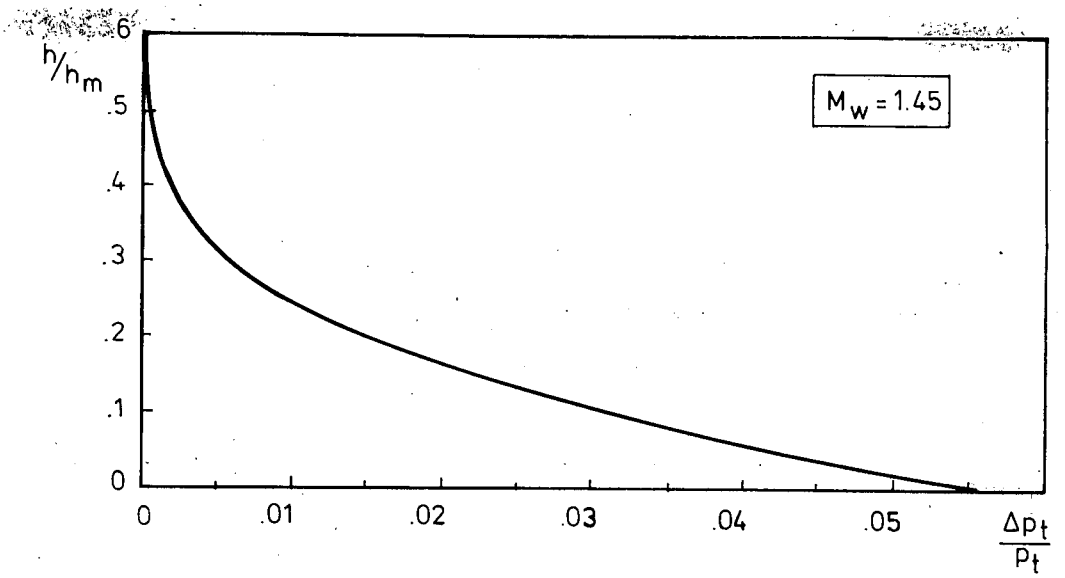

Fig. 6: Total pressure losses across shock wave in test section

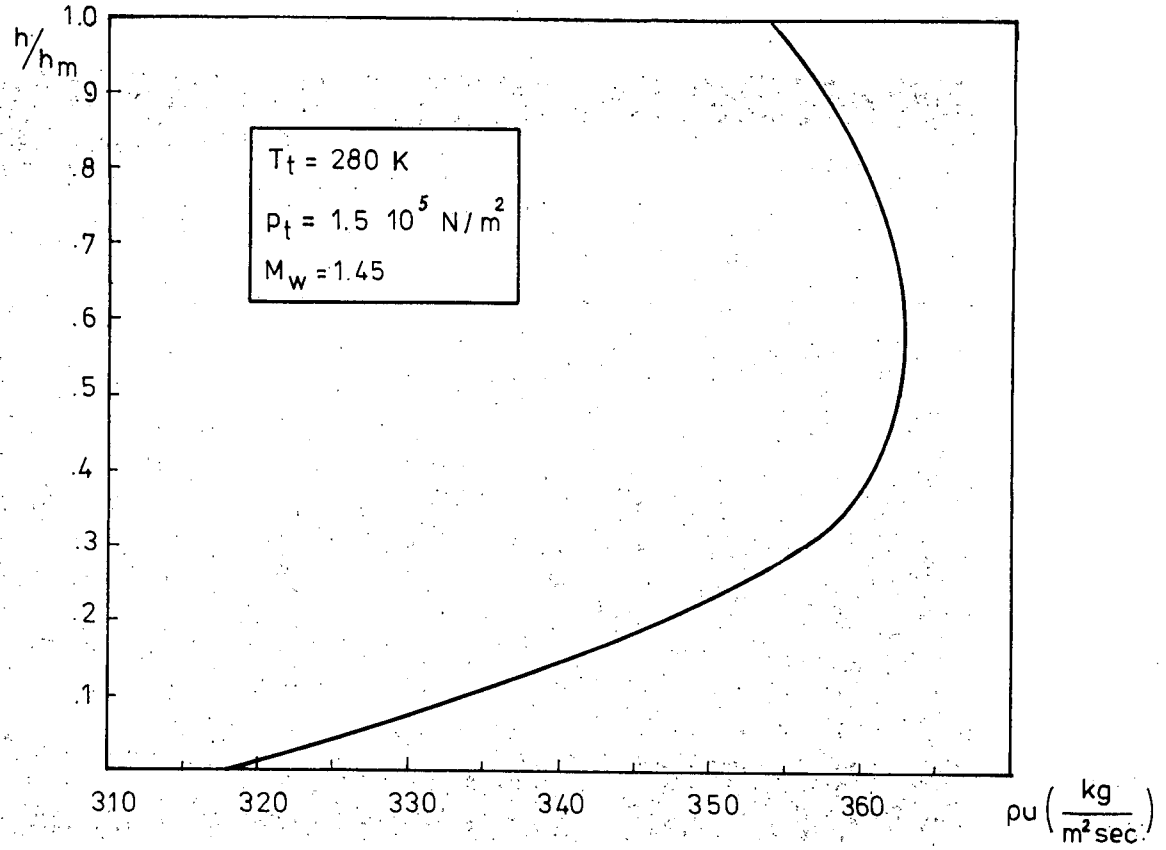

Fig.7: Specific mass flow through the test section

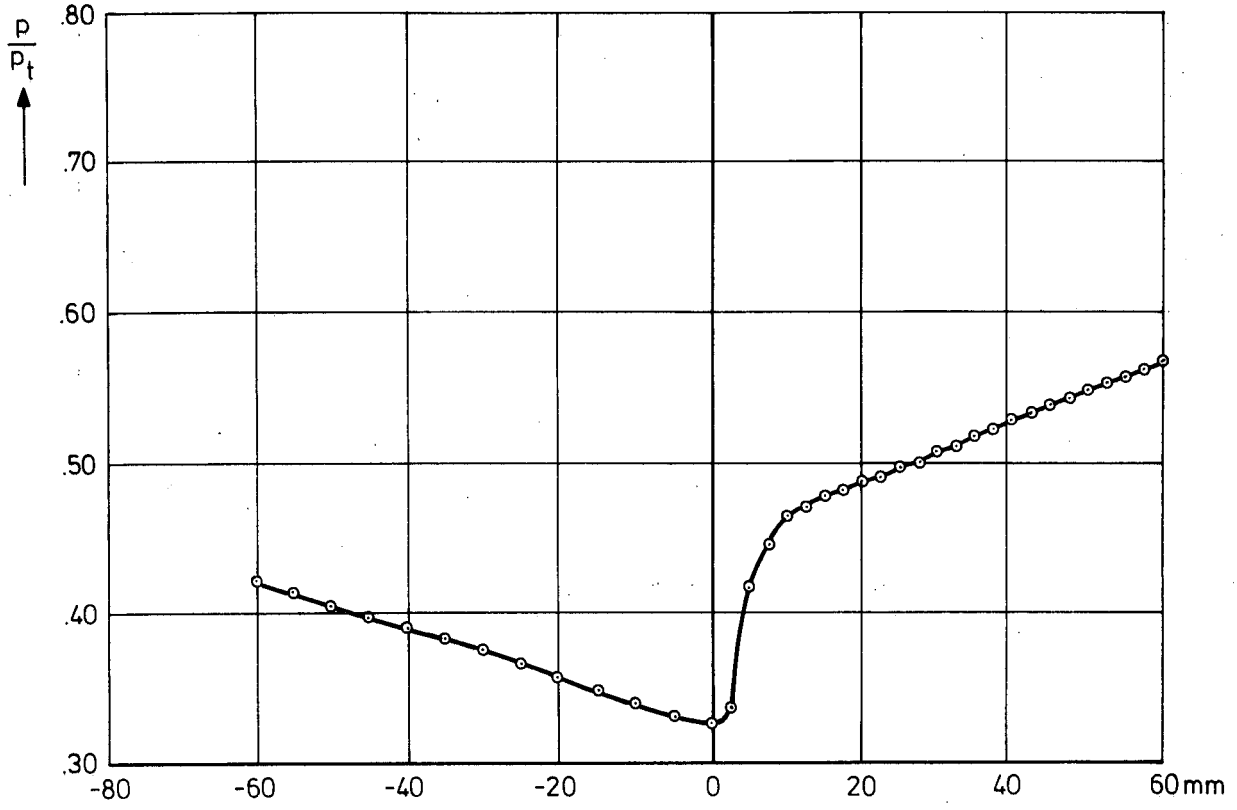

Fig. 8 : Surface pressure distribution.

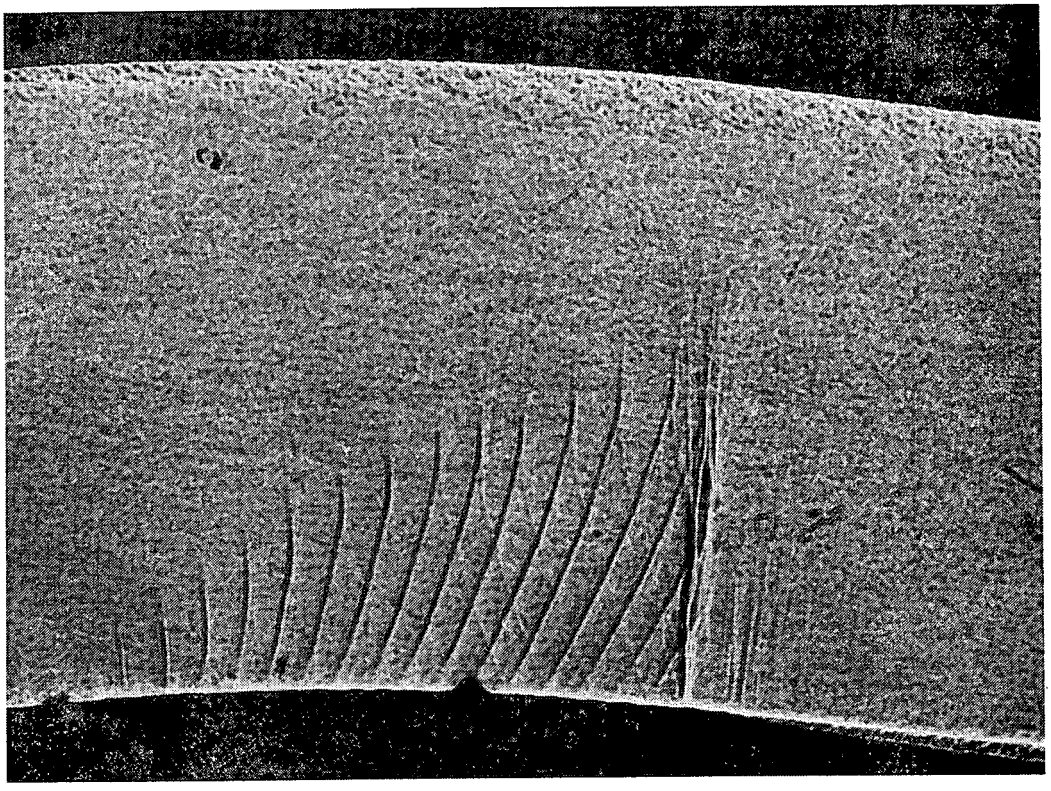

Fig. 9 : Schlieren picture of curved transonic flow.

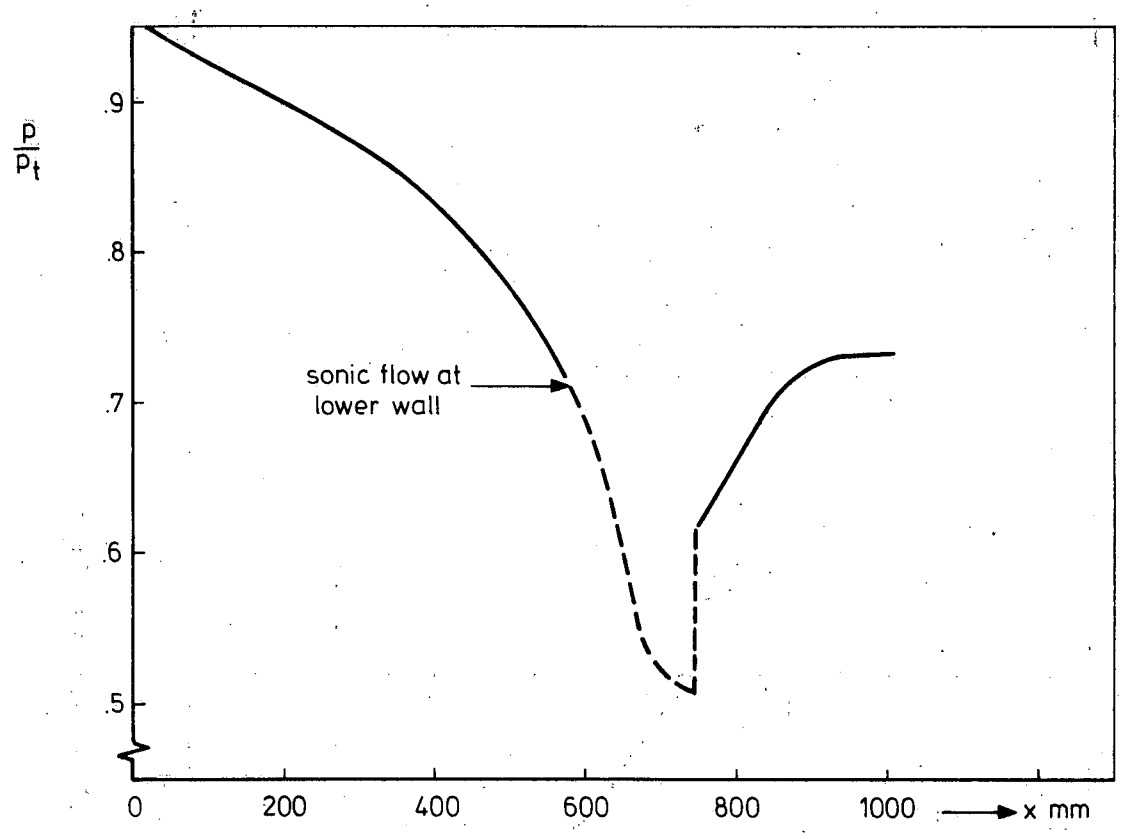

Fig.10 : Mean streamwise pressure distribution in the nozzle just in front of the shock wave.

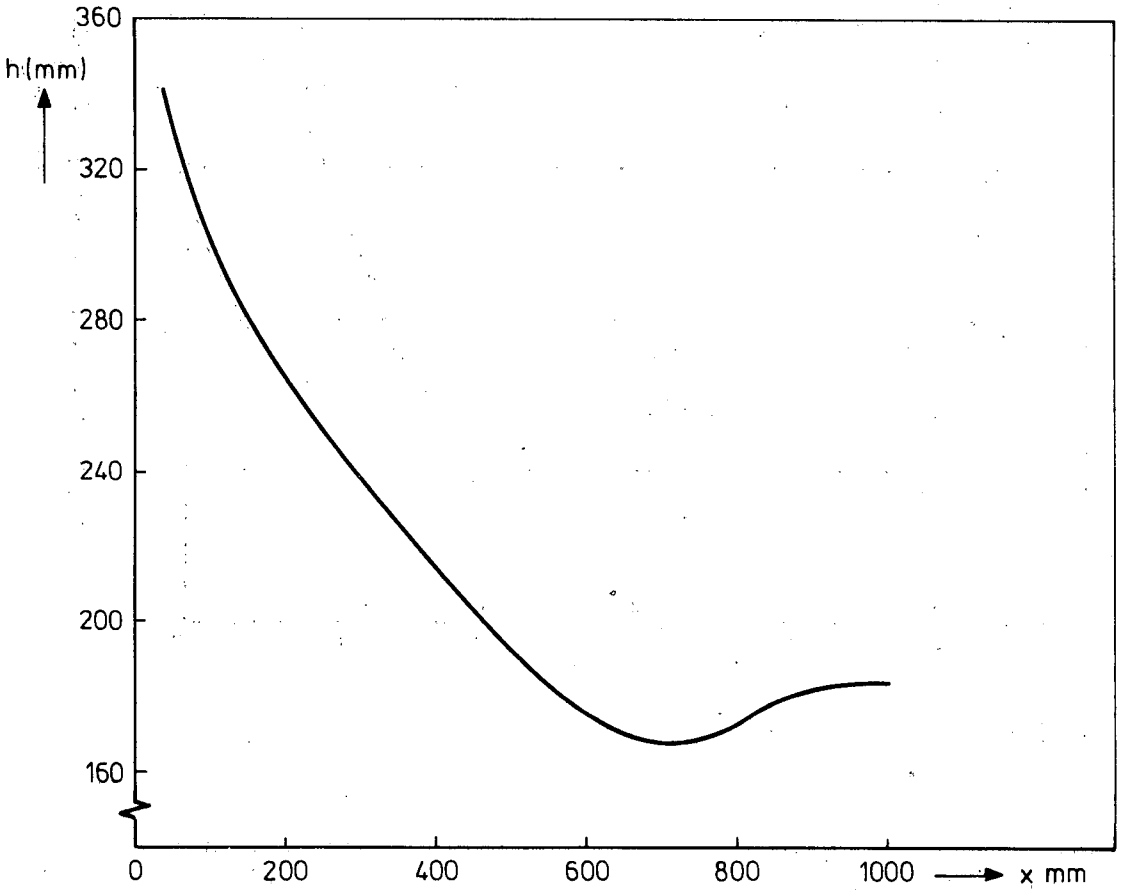

Fig.11 : Height of the nozzle in streamwise direction.

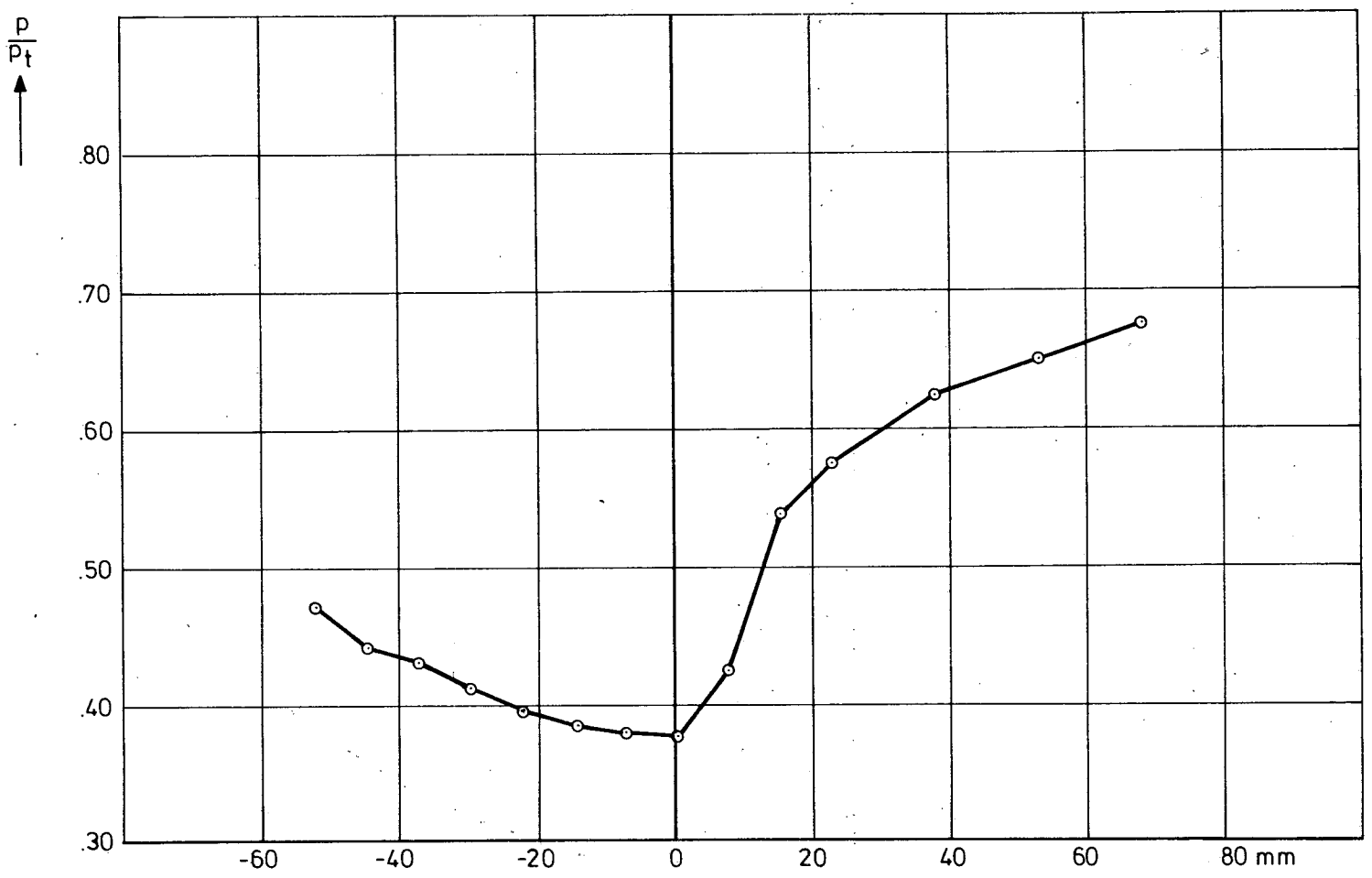

Fig. 12 : Measured surface pressure at a NACA-0012 profiel (chord 150 mm).

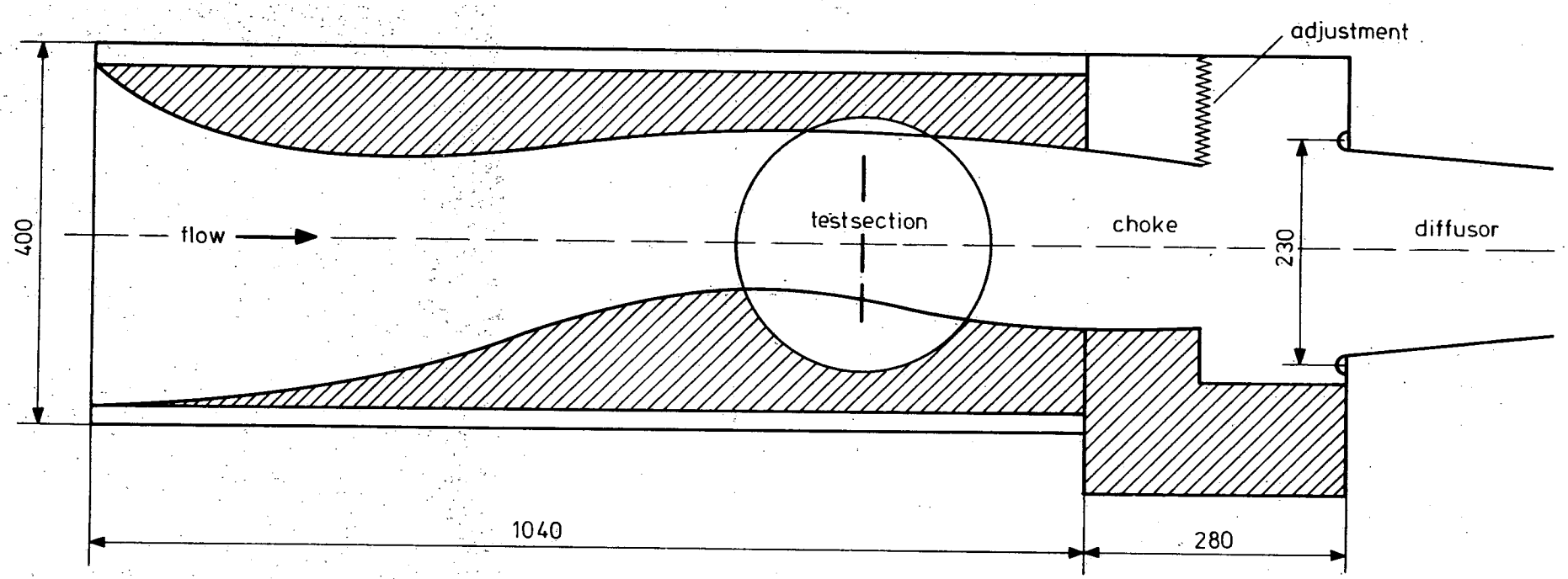

Fig. 13 : Scheme of nozzle showing test section and choke (dimensions in mm) .

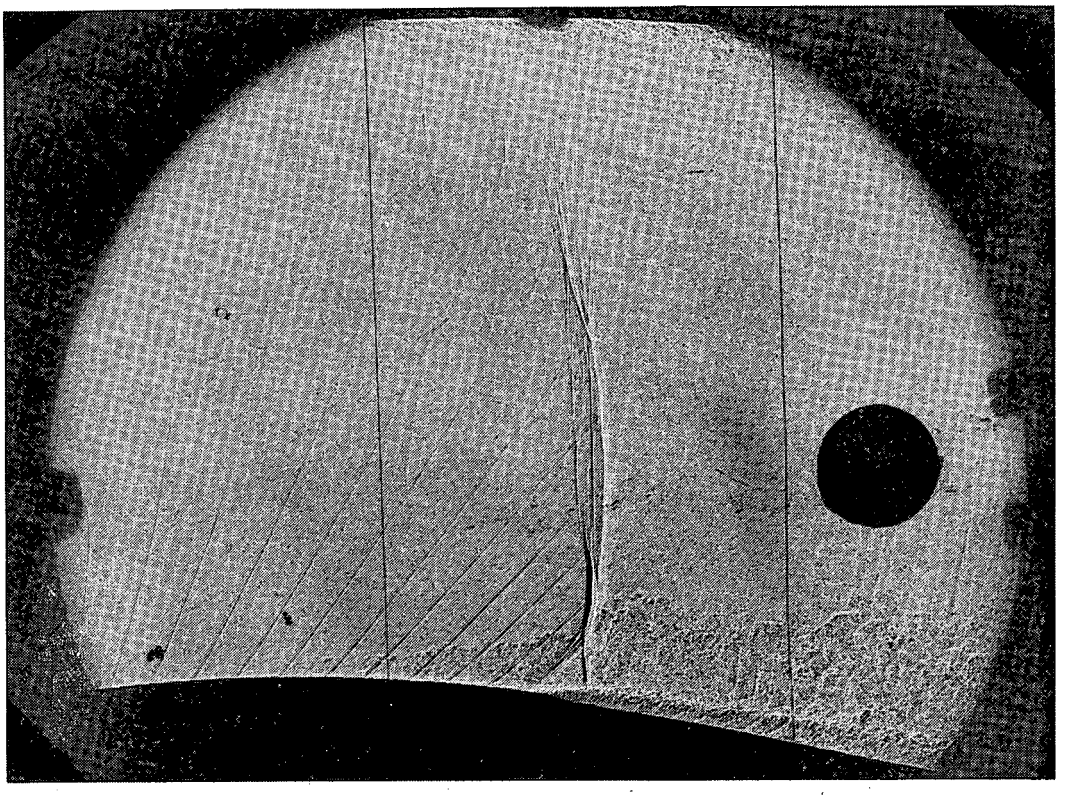

Fig. 14: Transonic shock wave-boundary layer interaction with artificial disturbances.

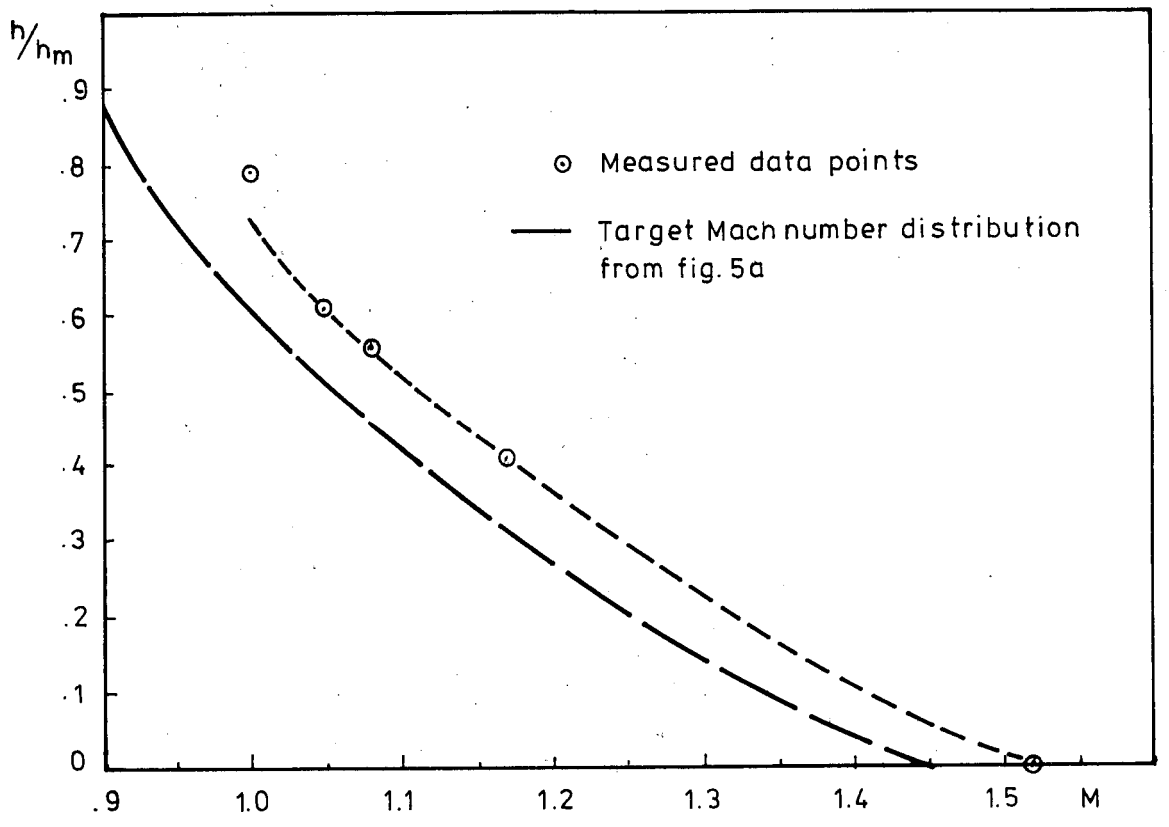

Fig. 15: Mach number distribution obtained from the intersection of disturbances in fig. 14.